J Nanopart Res (2013) 15:1488
DOI 10.1007/s11051-013-1488-6

RESEARCH PAPER

PAMAM dendrimer-coated iron oxide nanoparticles: synthesis and characterization of different generations

Rouhollah Khodadust · Gozde Unsoy · Serap Yalcın · Gungor Gunduz · Ufuk Gunduz

Received: 3 July 2012 / Accepted: 6 February 2013 / Published online: 19 February 2013

Abstract This study focuses on the synthesis and characterization of different generations (G_0–G_7) of polyamidoamine (PAMAM) dendrimer-coated magnetic nanoparticles (DcMNPs). In this study, superparamagnetic iron oxide nanoparticles were synthesized by co-precipitation method. The synthesized nanoparticles were modified with aminopropyltrimethoxysilane for dendrimer coating. Aminosilane-modified MNPs were coated with PAMAM dendrimer. The characterization of synthesized nanoparticles was performed by X-ray diffraction, X-ray photoelectron spectroscopy (XPS), Fourier transform infrared spectroscopy (FTIR), transmission electron microscopy (TEM), dynamic light scattering, and vibrating sample magnetometry (VSM) analyses. TEM images demonstrated that the DcMNPs have monodisperse size distribution with an average particle diameter of 16 ± 5 nm. DcMNPs were found to be superparamagnetic through VSM analysis. The synthesis, aminosilane modification, and dendrimer coating of iron oxide nanoparticles were validated by FTIR and XPS analyses. Cellular internalization of nanoparticles was studied by inverted light scattering microscopy, and cytotoxicity was determined by XTT analysis. Results demonstrated that the synthesized DcMNPs, with their functional groups, symmetry perfection, size distribution, improved magnetic properties, and nontoxic characteristics could be suitable nanocarriers for targeted cancer therapy upon loading with various anticancer agents.

Keywords Iron Oxide (Fe_3O_4) · Dendrimer · Magnetic nanoparticle · Cancer therapy

Abbreviations

MNPs	Magnetic nanoparticles, magnetite, Fe_3O_4
DcMNPs	Polyamidoamine (PAMAM) dendrimer-coated magnetic nanoparticles (DcMNPs)
APTS	Aminopropyltrimethoxysilane
XRD	X-ray diffraction
FTIR	Fourier transform infrared spectroscopy
TEM	Transmission electron microscopy
DLS	Dynamic light scattering
TGA	Thermal gravimetric analysis
VSM	Vibrating sample magnetometry
M_S	Saturated magnetization

R. Khodadust · G. Unsoy · U. Gunduz
Department of Biotechnology, Middle East Technical University, 06800 Ankara, Turkey

R. Khodadust (✉) · U. Gunduz (✉)
Department of Biological Sciences, Middle East Technical University, 06800 Ankara, Turkey
e-mail: raoul.1357@gmail.com

U. Gunduz
e-mail: ufukg@metu.edu.tr

S. Yalcın
Department of Food Engineering, Ahi Evran University, 40100 Kırşehir, Turkey

G. Gunduz
Department of Chemical Engineering, Middle East Technical University, 06800 Ankara, Turkey

Introduction

Magnetic particles (microspheres, nanospheres, and ferrofluids) are widely studied for their applications in biology and medicine such as enzyme and protein immobilization, magnetic resonance imaging (MRI), RNA and DNA purification, magnetic cell separation, and magnetically controlled delivery of anticancer drugs, as well as hyperthermia (Matsunaga et al. 1999; Bazylinski 1996; Taylor et al. 2000; Mornet et al. 2000; Reetz et al. 1998). These magnetic particles are generally composed of magnetite (Fe_3O_4) core and a polymeric shell where the drugs, nucleic acids, and proteins are bound. The shells such as dendrimers, dextran, PEG, and chitosan must be biocompatible, and possess active groups which can be conjugated to biomolecules such as proteins, enzymes, and drugs (Arias et al. 2001; Shimomura et al. 2003; Tanyolaç and Özdural 2000). Dendrimers are a relatively novel class of polymers with a well-defined, three-dimensional structure and are being used for modifying iron oxide magnetic nanoparticles (MNPs). The buildup of functional groups, symmetry perfection, nanosize, and internal cavities on dendrimer-modified MNPs makes them suitable for applications in gene therapy and cancer therapy.

Dendrimer-modified MNPs are good nonviral synthetic vectors and have the advantages of safety, simplicity of use, and ease of mass production compared with viral vectors which have inherent risk in clinical applications. They are synthesized through different cycles or ''generations'' by adding branched monomers that react with the functional groups of the core such as iron oxide nanoparticles after which the free end groups of monomers can further react. Thus, the number of terminal groups will increase after each generation of the synthesis (Pan et al. 2007; Gao et al. 2005; Acharya et al. 2009). Many commercial small molecule drugs with anticancer, anti-inflammatory, and antimicrobial activities have been successfully associated with dendrimers such as poly(amidoamine) (PAMAM), poly(propyleneimine), and poly (etherhydroxylamine), either via physical interactions or through chemical bonding (Svenson 2009). Dendrimers offer well-defined nanoscale architecture, multivalency, and structural versatility, leading to their emergence as a promising class of nanobiomaterials (Lee et al. 2005). One class of the dendrimers, PAMAM dendrimers, have been utilized as carriers of antiviral or anticancer agents and in vivo imaging molecules (Svenson and Tomalia 2005; Esfand and Tomalia 2001; Duncan and Izzo 2005). When PAMAM dendrimers are used as drug carriers, they can enhance the biodistribution of drugs and possibly take advantage of enhanced permeation and retention effect for targeting tumors (Sato et al. 2001; Malik et al. 2000; Matsumura and Maeda 1986). In addition, it was demonstrated that the dendrimer surfaces can be modified with ligands to target specific tissues and tumors, thus capable of active receptor targeting (Kukowska-Latallo et al. 2005). The dendritic carriers should eventually release the drugs loaded onto them in a well-defined and favorable rate. The release rates are dependent on the type of chemical bond between the drug and its carrier as well as the nanoscale structure of the dendrimer conjugate and steric effects. Several dendrimers have been investigated as drug carriers for various cancer drugs (Malik et al. 1999; Zhuo et al. 1999; Gurdag et al. 2006; Lee et al. 2006). PAMAM dendrimers are hydrophilic, biocompatible, monodisperse, and cascade-branched macromolecules with highly flexible surface chemistry that facilitates functionalization (Stiriba et al. 2002; Shukla et al. 2005; Hong et al. 2004; Thomas et al. 2004). They can be used as uniform scaffolds carrying multiple copies of biologically relevant molecules without interfering with the components' functions (Esfand and Tomalia 2001; Majoros et al. 2003). The PAMAM coating reduces magnetite agglomeration, and the increased cationic contribution will be useful for generating a colloidal suspension with increased surface area (Liu et al. 2011). PAMAM dendrimers can introduce a dense outer amine shell through a cascade-type generation (Tomalia et al. 1985). The terminal amine groups of PAMAM dendrimers can be modified and linked with various biomolecules such as drugs, vitamins (folic acid, biotin etc.), antibodies, and imaging agents (Takeda et al.2003; Shukoor et al. 2007; Menjoge et al. 2010). In general, dendrimers possess empty internal cavities and can encapsulate different drug molecules (Hansson and Edfeldt 2005; Du et al. 2000). It was well established that the conjugation of special targeting moieties to dendrimers can lead to preferential distribution of the cargo in the targeted tissue or cells.

In this study, various generations of dendrimer-coated magnetic nanopartices were synthesized and they were characterized by XRD, FTIR, TEM, VSM,

XPS, and DLS analyses. Cellular internalization and cytotoxic properties of the nanoparticles were also reported. The results demonstrated that the synthesized nanoparticles could be promising carriers for anticancer agents in targeted cancer therapy.

Experimental

Materials

Ferric chloride hexahydrate ($FeCl_36H_2O$), ferrous chloride tetrahydrate ($FeCl_24H_2O$), 32 % ammonia solution (NH_3), 3-aminopropyltrimethoxysilane ($NH_2(CH_2)_3$–Si–$(OCH_3)_3$, APTS), methyl acrylate, methanol, ethanol, and ethylenediamine were purchased from Sigma Aldrich.

Preparation of magnetic nanoparticles

The MNPs (Fe_3O_4) were prepared with a minor modification of co-precipitation method. 1.6133 g $FeCl_24H_2O$ and 2.6279 g $FeCl_36H_2O$ (Fe_2^+, Fe_3^+ = 1:2) were dissolved in 150 ml of distilled water under nitrogen environment, and 35 ml of ammonia solution was added slowly with vigorous stirring mechanically at 2000 rpm for 2 h. During the reaction, temperature was kept at 90 °C. The black precipitate was washed five times with distilled water and five times with ethanol using magnetic separation. The obtained iron oxide nanoparticles were dispersed in ethanol at 5 g l^{-1} (Pan et al. 2007; Gao et al. 2005, Unsoy et al. 2012).

Preparation of APTS-coated magnetic nanoparticles

Surface modification of Fe_3O_4 was performed with 3-aminopropyltrimethoxysilane (APTS). Ethanol (125 ml) was added into the 25 ml of Fe_3O_4-ethanol solution (5 g l^{-1}) and sonicated with ultrasonicator (Bandelin Sonopuls ultrasonic homogenizer HD 2200) for 30 min, and 10 ml APTS was added to the mixture at the 20th min of sonication. Then, the mixture was stirred with mechanical stirrer at room temperature for 15 h. The resulting black precipitate was separated by magnetic decantation and washing with methanol for several times. The obtained nanoparticles modified with APTS are called G_0 generation (Pan et al. 2007; Gao et al. 2005).

Surface coating using PAMAM dendrimer

Surface coating of G_0 generation of nanoparticles was carried out with PAMAM dendrimer through Michael reaction. Methyl acrylate/methanol solution (20 %, v/v) was added (200 ml) to the obtained G_0 generation, and the suspension was sonicated in an ultrasonic water bath at room temperature for 7 h. After ultrasonication, nanoparticles were eluted by magnetic decantation and washed with methanol. Ethylenediamine methanol solution (50 %, v/v) was added (40 ml), and suspension was sonicated for 3 h. The particles were washed with methanol. The stepwise growth of dendrimers was repeated, until the preferred number of generation (G_1–G_7) was achieved using the methyl acrylate and ethylenediamine (Fig. 1). The product was then washed three times with 25 ml methanol and five times with 25 ml water by magnetic decantation (Pan et al. 2007; Gao et al. 2005).

Cellular internalization of dendrimer-coated magnetic nanoparticles

The internalization of dendrimer-coated iron oxide nanoparticles were shown by light and confocal microscopy. The nanoparticles were incubated with breast cancer MCF-7 cell lines in 6 well plates. After 24 h incubation, the medium was removed from the plates and the plates were washed with PBS for several times so that all free DcMNPs were removed from the environment. Their photographs were taken under an inverted optical microscope to determine cellular internalizations of DcMNPs (Wuang et al. 2007; Mahmoudi et al. 2009). In addition, G_4DcMNPs were conjugated with fluorescein isothiocyanate (FITC) in EDC/NHS solution which were applied onto the MCF-7 cells. The conjugation process was carried out using the surface activation method by EDC–NHS chemistry (Acharya et al. 2009). 20 mg EDC and 4.6 mg NHS were dissolved in 2 ml of PBS (pH 5.8) followed by the addition of 100 µl of FITC in the suspension. After 2 h, 5 mg ml^{-1} of G_4DcMNPs was added to the above solution and left to remain at 4 °C under continuous magnetic stirring for over night. Then, product was washed three times with PBS by magnetic decantation. The resultant FITC-conjugated MNPs were visualized by confocal microscopy.

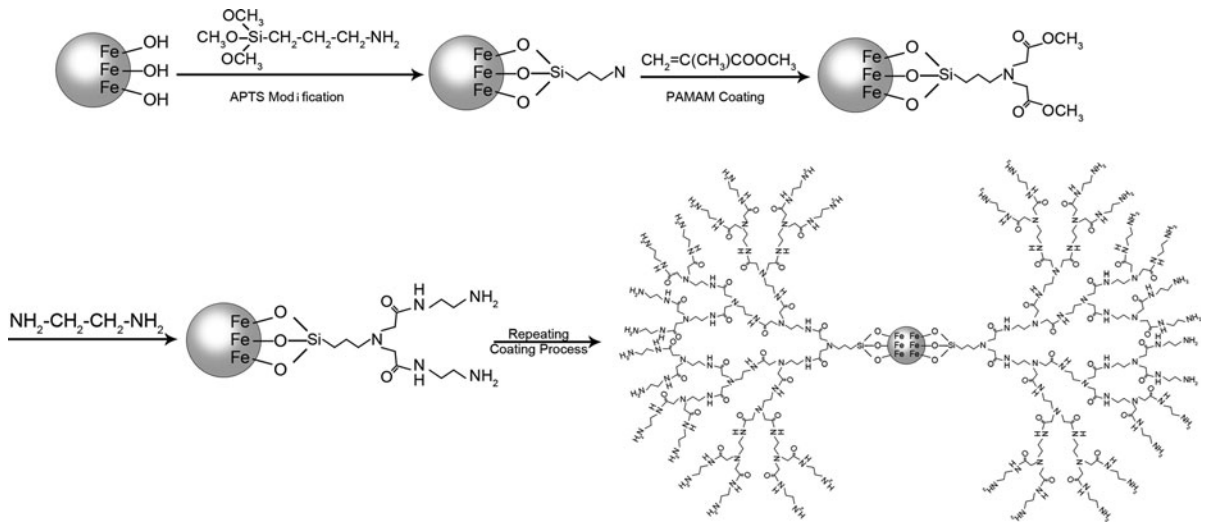

Fig. 1 Stepwise modification of iron oxide nanoparticles with APTS, dendrimer-coating processes

Cytotoxicity of dendrimer-coated magnetic nanoparticles

MCF-7 cells were grown in 75-ml culture flasks in RPMI/1640 medium supplemented with 10 % FBS, and 0.2 % gentamycin solution at 37 °C under 5 % CO_2. The cells were subcultured 2–3 times per week with 0.25 % trypsin–EDTA. Antiproliferative effects of dendrimer-coated nanoparticles on MCF-7 cells were evaluated by means of the Cell Proliferation Kit (Biological Industries) according to manufacturer's instructions. Assay was a colorimetric test based on the reduction tetrazolium salt, XTT, to colored formazan products by mitochondria of live cells. Then, XTT reagent was added, and soluble product was measured at 500 nm with an Spectromax 340, 96-well plate reader (Molecular Devices, USA).

Results

Synthesis of magnetic nanoparticles

Temperature of the reaction system and ammonia addition rates are two important factors that influence the synthesis of MNPs. In order to synthesize nano-sized, crystalline, bare iron oxide particles, these two parameters were tested. Iron oxide nanoparticles synthesized at different temperatures between 20 and 90 °C. XRD results demonstrated that the nanoparticles with preferred crystalline structure were obtained at 90 °C. The time of ammonia addition was also optimized. When the ammonia was added very slowly, smaller nanocrystals were synthesized, so that the size can be adjusted.

Aminosilane modification of nanoparticles

Optimizing sonication time during aminosilane modification improves magnetic properties and size distribution. Bare nanoparticles were modified with APTS to prepare them for dendrimer coating. The sonication time was optimized to obtain DcMNPs with desired size and shape. The magnetic properties of APTS-modified nanoparticles were improved when the time of sonication was increased from 10 to 30 min, and APTS was added to the reaction at the 20th min of sonication. Optimizations in aminosilane modification method decreased the agglomeration of nanoparticles, resulted in the synthesis of DcMNPs with desired size distribution, and improved magnetic properties.

X-ray diffraction analysis (XRD)

Bare iron oxide nanoparticles synthesized at different temperatures between 20 and 90 °C, and X-ray powder diffraction analyses of synthesized nanoparticles were performed to identify the crystal structure. It was observed that the highest crystalline structure

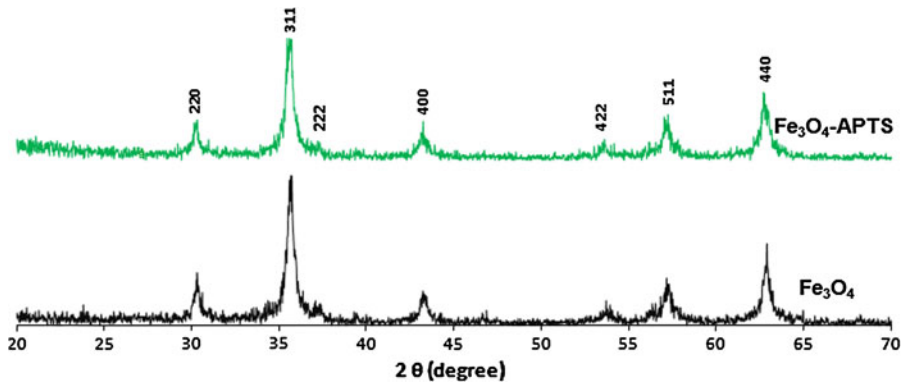

Fig. 2 X-Ray powder diffraction of Fe_3O_4 and Fe_3O_4-APTS nanoparticles

was achieved at 90 °C. Up to 50 °C, the synthesized iron oxide nanoparticles show amorphous or noncrystalline solid characteristics. At temperatures greater than 50 °C, the nanoparticles started to show crystalline characteristics. XRD pattern of Fe_3O_4 nanoparticles synthesized at 90 °C appeared with diffraction peaks of (220), (311), (400), (422), (511), (440), and (533), which are the characteristic peaks of the magnetite crystal having a cubic spinal structure. Coating of nanoparticles with PAMAM dendrimers G_5–G_7 did not change the characteristic XRD pattern (Fig. 2).

Fourier transform-infrared spectroscopy (FT-IR)

FTIR results related to bare MNP, MNP-APTS, and G_1–G_7 generation of dendrimer-modified MNPs are given in Fig. 3.

The presence of Fe_3O_4 core could be identified by the strong stretching absorption band between 408 and 673 cm^{-1}, which correspond to the Fe–O bond of nanoparticles (Julian et al. 1991).

IR analysis of aminosilane, methanol, and methylacrylate were seperately performed (data not shown). Considering magnetite (Fe_3O_4) Fe–O group bond observed at 570 cm^{-1} which corresponds to intrinsic stretching vibration of the metal at tetrahedral site (Fe_{tetra}–O). The vibration of NH_2 group is at around 3410 cm^{-1}. The stretching vibration of Si–O–Fe is at 950 cm^{-1}, which shifts to about 1050 cm^{-1} for G_7 nanoparticles because of the presence of highly electronegative –CO–NH_2 groups. C–H bonds present in methylacrylate, aminosilanes, and methanol, and the related bonds, can be seen at 2840, 3910, and 3010 cm^{-1}, respectively. Vibration of –CO–NH– bonds were observed at 1450, 1490, 1530, and 1620 cm^{-1}. O–H bonds related to alcohols were at 3200–3600 cm^{-1} [32]. FT-IR spectra is compatible with the stepwise dendrimer modification process.

Transmission electron microscopy analysis (TEM)

It is known that the size distribution smaller than 30 nm is the characteristics of superparamagnetic iron oxide nanoparticles. On analyzing the TEM results (Fig. 4), it was understood that the sizes of obtained bare iron oxide MNPs were 8 ± 5 nm. This shows that the synthesized MNPs are potentially superparamagnetic. However; in order to confirm this, vibrating sample magnetometer analysis was done.

TEM image of aminosilane-modified nanoparticles demonstrated that the size distribution of aminosilane-modified MNPs was more uniform. The size change was around 1 nm after modification with aminosilane which was observable on the surface of nanoparticles.

Dynamic light scattering analysis (DLS)

The average diameters of bare MNPs were found as 55 ± 15 nm in DLS measurements (Fig. 5a). The average diameters of the dendrimer-coated MNPs (G_7DcMNP) were 45 ± 10 nm in DLS measurements (Fig. 5b).

Zeta (ζ) potential analysis

The ζ potential values of bare MNPs were calculated as −23.2 mV in PBS buffer pH 7.2. The ζ potentials of

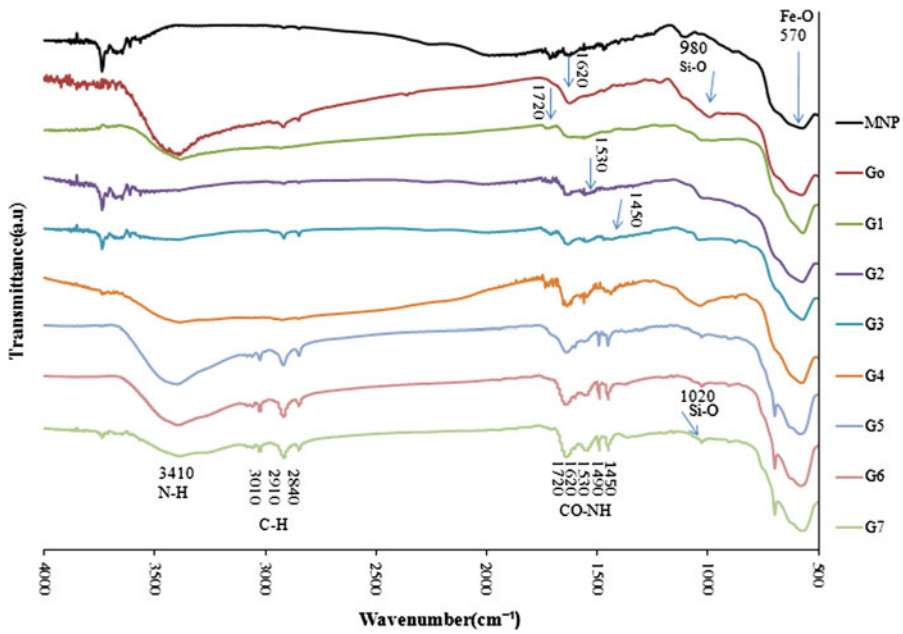

Fig. 3 FT-IR results related to MNP, MNP-APTS, and G_1–G_7 generations of dendrimer-modified magnetic nanoparticles

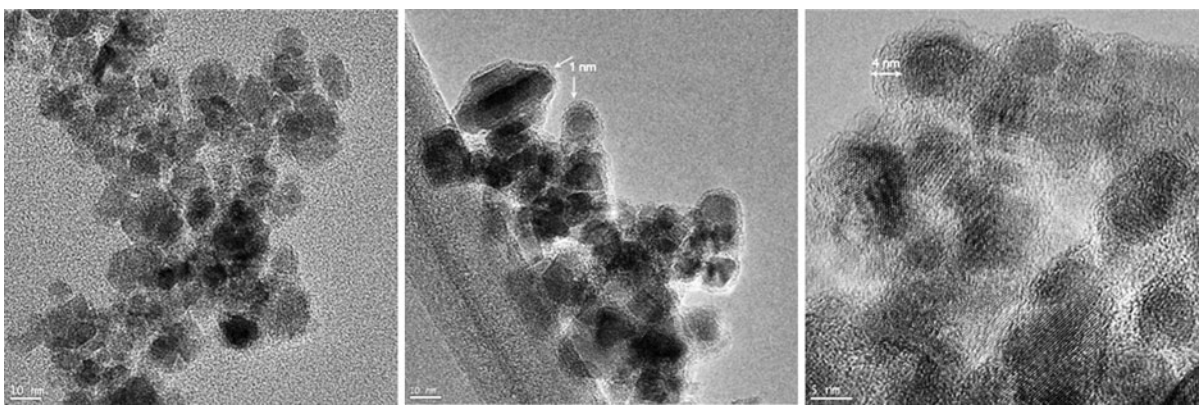

Fig. 4 The sizes of obtained G_7 generation DcMNP were 16 ± 5 nm. The change of the size after dendrimer modification was around 8 nm

G_5DcMNPs and G_7DcMNPs were observed at +15.1 and +20.9 mV, respectively.

Vibrating sample magnetometer analysis (VSM)

The applied magnetic field was changed and magnetization properties of synthesized Fe_3O_4, aminosilane-modified MNPs, and DcMNPs were measured at 25 and 37 °C. Magnetization curves of the MNPs, APTS-modified MNPs, and DcMNPs at 37 °C are given in Fig. 6. Magnetic materials showing a superparamagnetic behavior have zero value of remanence and coercivity. The remanence and coercivity observed in the hysteresis loops of MNPs, APTS-coated MNPs, and DcMNPs both at 25 and 37 °C were negligible. VSM results of bare MNPs analyzed at 25 and 37 °C were obtained as 54.5 and 48.8 emu g^{-1} respectively.

In order to determine the magnetic characteristics of synthesized nanoparticles, VSM analysis was done at body temperature and room temperature. The maximum magnetization were found to be 48.8, 61.4, 53.4, and 51.1 emu g^{-1} for MNP, APTS-coated

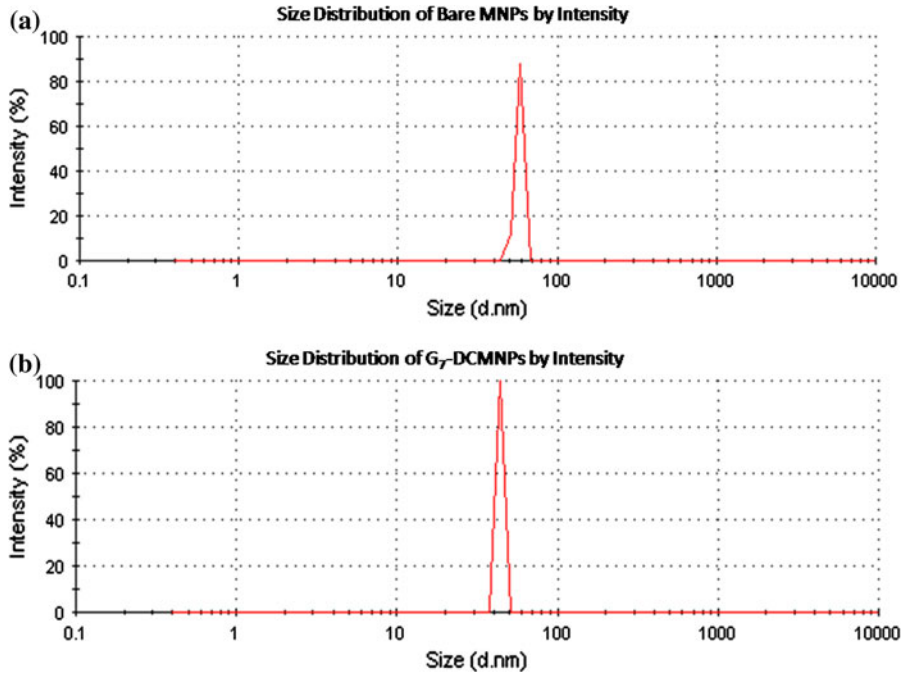

Fig. 5 Dynamic light scattering *graphs* of bare MNPs (**a**) and G_7DcMNPs (**b**)

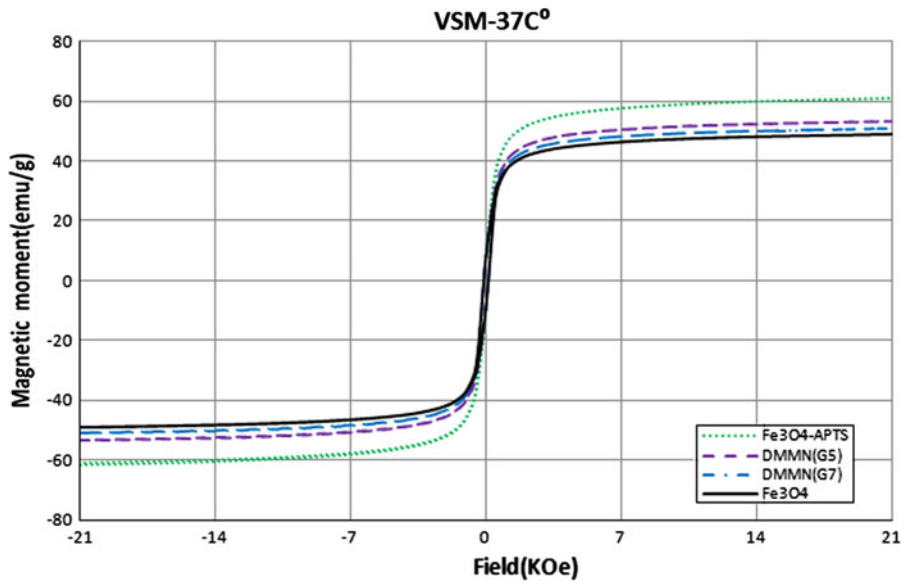

Fig. 6 Magnetization curve of the MNPs, APTS-modified MNPs, and DcMNP at 37 °C

MNP, DcMNPsG_5, and DMMNsG_7, respectively, at 37 °C. The maximum magnetizations at room temperature were found to be 54.5, 56.5 and 49.5 emu g^{-1} for MNP, APTS-coated MNP and DMMNsG_5, respectively (data not shown) .

Thermal gravimetric analysis (TGA-FTIR)

The TGA curve of bare, aminosilane-modified and dendrimer-coated MNPs (Fig. 7) shows that the weight loss of bare MNPs over the temperature range

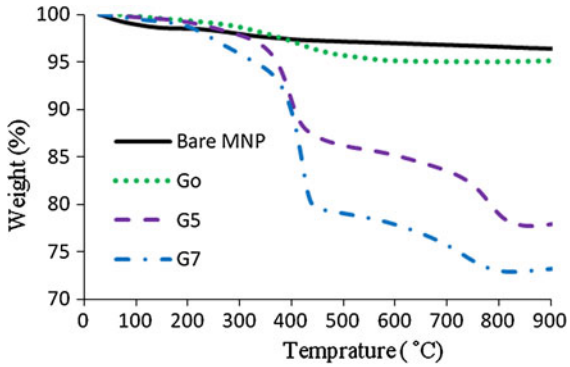

Fig. 7 The TGA *curve* of bare, aminosilane-modified, and dendrimer-coated MNPs

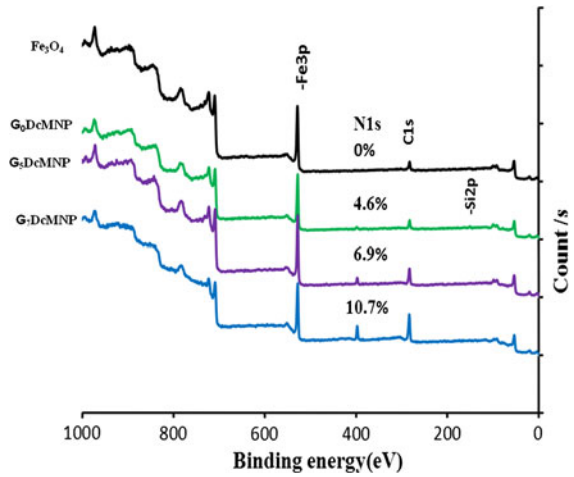

Fig. 8 General XPS scanning spectrum belonging to the surfaces of bare MNP, G_0, G_5, and ve G_7 nanoparticles

from 30 to 850 °C is about 3.5 % which might be because of the loss of residual water in the sample. In aminosilane-modified MNPs, the weight loss is about 5 % which reflects the amount of APTS at the surface of nanoparticles (1.5 % aminosilane and 3.5 % water loss in the sample). The fifth (G_5DcMNP) and seventh (G_7DcMNP) generations of dendrimer-coated MNPs had 22 and 27 % weight losses, respectively, indicating the amount of PAMAM dendrimer layers on the surfaces of nanoparticles.

TGA analysis shows that there was an increase in the organic content of MNPs when the growth of the PAMAM dendrimer was increased to higher generations.

X-ray photoelectron spectroscopy (XPS)

Qualitative and quantitative surface characterizations of synthesized bare MNP, G_0, G_5, and G_7 nanoparticles have been done by X-ray photoelectron spectroscopy (XPS). Figure 8 shows the general XPS scanning spectra of bare MNP, G_0, G_5, and G_7 nanoparticles. The peaks obtained upon XPS analysis were belonging to Si 2p (100.3 eV), C 1s (284.2 eV), N 1s (398.2 eV), O 1s (528.5 eV), and Fe 2p (710.3 eV). N 1s and Si 2p peaks belonging to nitrogen and silane were not present in the spectrum of bare MNPs as expected.

The regional XPS scans were also performed for the quantitative analyses of various atoms (Si, N, C, O, and Fe) found in nanoparticles. As seen in Fig. 8, there was a decrease in the oxygen (O 1s) and iron (Fe 2p) contents in G_0, G_5, and G_7 nanoparticles due to the increase in the thicknesses of PAMAM layers at the surfaces of nanoparticles. The peaks of Si 2p (100.3 eV) and Fe 2p (398.2 eV) were observed in the nanoparticles after the aminosilane modification. During the synthesis of each generation of dendrimer at the surface of the nanoparticles, ramifying occurs, which results in an exponential increase on the amount of free surface atoms. The exponential increase of nitrogen and carbon atoms were observed in XPS spectra of G_0, G_5, and G_7 nanoparticles. The amount of nitrogen and carbon at the surface of G_0, G_5, and G_7 dendrimer-coated nanoparticles were counted as 4.6, 6.9, and 10.7 % for nitrogen; and 18.6, 27.6, and 42.8 % for carbon, respectively (Table 1). These results demonstrate that the PAMAM dendrimer coating was achieved successfully.

Cellular internalization of dendrimer-coated magnetic nanoparticles

It was demonstrated by inverted light microscopy that while none of the bare MNPs was taken up by the cells, most of the DcMNPs were internalized (at 37 °C, 2 h). G_4DcMNPs containing MCF-7 cells are shown in Fig. 9. Moreover G_4DcMNPs were conjugated with FITC (fluorescein isothiocyanate). The resultant FITC-conjugated MNPs were visualized by confocal microscopy (Fig. 10).

The results are promising because nanoparticles can be internalized into the cells even if they are applied at low concentrations and cell viability was not affected. Cellular internalization was carried out at five different concentrations of DcMNPs.

Table 1 Atomic percentage changes in bare iron oxide, aminosilane-modified, G_5 and G_7DcMNPs

MNP	Fe_30_4 (%)	G_0DcMNP (%)	G_5DcMNP (%)	G_7DcMNP (%)
N ls (% of nitrogen atom)	0	4.6	6.9	10.7
C ls (% of carbon atom)	18.2	18.6	27.6	42.8
Fe 2p3 (% of iron atom)	21.6	21.5	18.7	11.8
Ol s (% of oxygen atom)	60.2	54.2	46.0	34.2
Si 2p	0	1.1	0.8	0.5

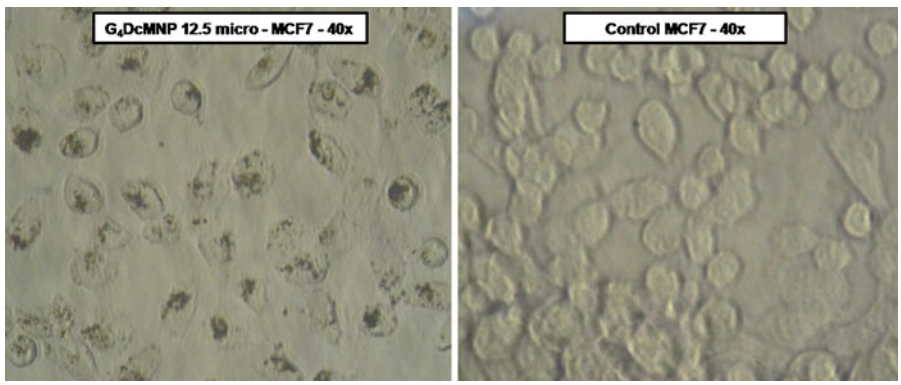

Fig. 9 Cellular internalization of dendrimer-coated magnetic nanoparticles by inverted light scattering microscopy (×40)

Cytotoxicity of dendrimer-coated nanoparticles

Cytotoxicity of DcMNPs was investigated by XTT cell proliferation assay. Survival rates indicated that there is no significant cytotoxic effect of the nanoparticles on MCF-7 cells.

Discussion

In this study, bare iron oxide nanoparticles were synthesized and coated with PAMAM to obtain different generations (G_1–G_7) of DcMNPs. Different parameters were optimized to synthesize DcMNPs with desired properties suitable for biomedical applications and drug delivery.

Bare nanoparticles were synthesized at different temperatures and different rates of ammonia addition. X-ray diffraction analysis proved that the synthesized MNPs at 90 °C were corresponding to the characteristics of pure magnetite crystal (Fe_3O_4) having a cubic spinel structure (Fig. 2).

In the FT-IR spectrum of synthesized MNPs (Fig. 3), Fe–O bond was observed at 570 cm^{-1} belonging to magnetite (Fe_3O_4). The stretching vibrations of Si–O–Fe and –CO–NH– bonds were observed at 980 and 1620 cm^{-1} after aminosilane modification. In dendrimer-coated MNPs; stretching vibration of Si–O-Fe shifts to left side around 1020 cm^{-1} for G_7 nanoparticles because of the presence of highly electronegative -CO-NH_2 groups. The new bonds of –CO–NH– were observed after synthesis of each dendrimer generations. Additional peaks were observed for vibrations of –CO–NH– in G_1DcMNP at 1720 cm^{-1}, G_2DcMNP at 1530 cm^{-1}, and G_3DcMNP at 1450 cm^{-1} (Julian et al. 1991). FT-IR spectra of magnetite, aminosilane-modified magnetite, and different generations of dendrimer-coated magnetite nanoparticles were compatible with the stepwise aminosilane modification and dendrimer-coating processes.

The particle sizes of iron oxide nanoparticles and dendrimer-coated nanoparticles visualized by TEM were in the range 3–13 and 11–21 nm, respectively (Fig. 4). The size change of G_1DcMNP was around 8 nm after coating with PAMAM dendrimer. It was also demonstrated that the diameters of PAMAM dendrimers increase systematically at a rate of approximately 1 nm per generation (Svenson and Tomalia 2005).

The hydrodynamic diameters of dendrimer-coated nanoparticles were obtained as 45 ± 10 nm with a

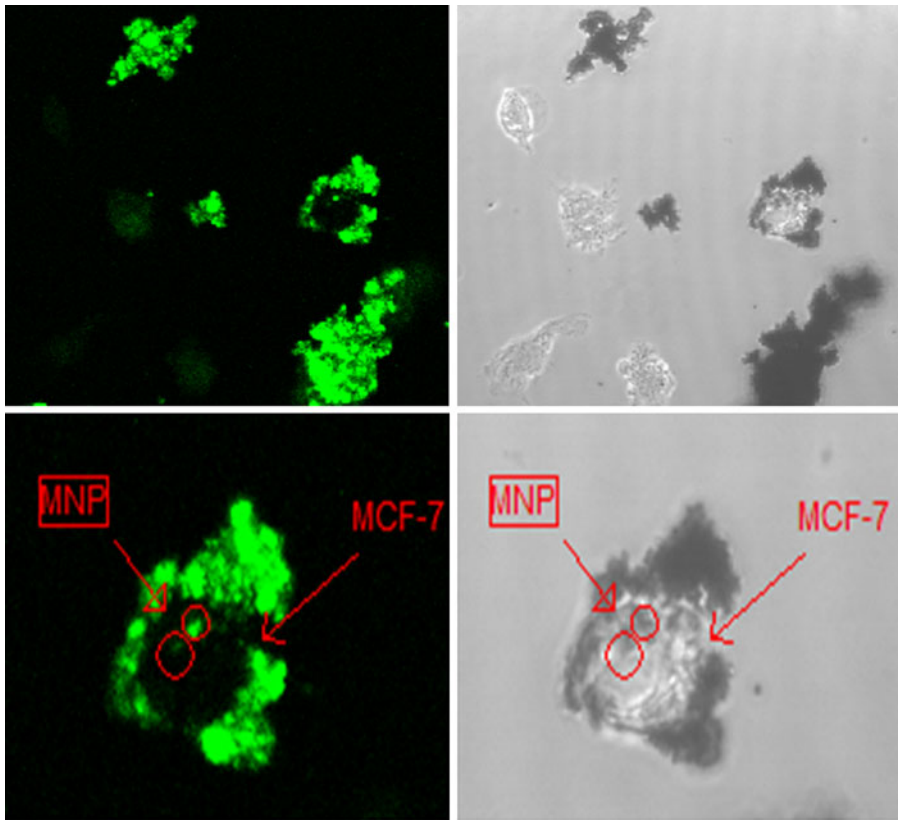

Fig. 10 Cellular internalization of FITC binding dendrimer-coated magnetic nanoparticles by confocal microscopy (×40)

smaller size distribution than the value obtained for bare nanoparticles, which is 55 ± 15 in DLS measurements. The higher value of average size obtained in DLS (compared to TEM) arises because DLS measures the hydrodynamic radii of the particles, which include the solvent layer at the interface (Rahman et al. 2012).

The agglomeration rate was very high in the bare Fe_3O_4 nanoparticles, which was also observed in DLS results and TEM images. The agglomeration occurs by the Van der Waals forces between the nanoparticles (Hoa et al. 2009). One of the effective approaches for preventing particle agglomeration is to coat nanoparticles with polymers or other targeting agents, such as dendrimers taking into account their biocompatibility (Durmus et al. 2009). Since the dispersity of nanoparticles was improved after the aminosilane modification and dendrimer-coating processes, the agglomeration of dendrimer-coated nanoparticles was expected to be reduced (Hoa et al. 2009). A PAMAM coating was used to reduce magnetite agglomeration. The agglomeration of DCMNPs was reduced by increasing dendrimer layers at the surface of bare MNPs as observed in DLS and TEM results (Uzun et al. 2010) .

The ζ potential values of bare MNPs were calculated as −23.2 mV in PBS buffer pH 7.2, because of the plentiful OH^- ions. The ζ potential values of G_5DcMNPs and G_7DcMNPs were observed at +15.1 and +20.9 mV, respectively. This increase in ζ potential value is due to increase in positive charge of $-NH_3^+$ on the MNP surface through dendrimerization which also proves the success of PAMAM-coating process (Pan et al. 2007).

Magnetic saturation value of the MNPs decreases as the size increases (Fig. 6), which agrees with the literature (Rahman et al. 2012).The decrease in the magnetic properties of the larger particles would be due to the increase in the volume/surface ratio in larger particles. Normally, we expect a reduction in magnetization of MNPs after modification with APTS. However, 5 % increase in magnetization of APTS-modified MNPs was observed when the magnetization

time was 10 min. Increasing the sonication time to 30 min and addition of APTS at the 20th min of sonication 20.5 % increase in magnetization was found. Increasing the time of ultrasonication and addition of APTS during sonication prevented the agglomeration of nanoparticles which resulted in the improvement of magnetic properties and size distribution. VSM results of bare MNPs analyzed at 25 and 37 °C were obtained as 54.5 and 48.8 emu g^{-1}, respectively, which indicates a 10 % reduction in the magnetic strength of MNPs at body temperature.

The TGA curves of bare MNPs, G_0DcMNPs, G_5DcMNPs, and G_7DcMNPs points out the weight loss of nanoparticles at high temperatures (Fig. 7). The results indicate that 17 % of the sample mass belongs to the dendrimer coating of fifth generation. Similarly, 22 % of the sample mass belongs to dendrimer coating of seventh generation. The increase in the organic content of nanoparticles observed in TGA analyses were the evidence of dendrimer growth when the PAMAM dendrimer coating was increased from G_5 to G_7.

General XPS scanning spectra of bare MNPs, G_0DcMNPs, G_5DcMNPs, and G_7DcMNPs demonstrated that peaks belonging to nitrogen and silane were not present in the spectrum of bare MNPs. These peaks were observed after aminosilane modification (Fig. 8).

In the regional XPS scanning spectra of G_0DcMNPs, G_5DcMNPs, and G_7DcMNPs, the amounts of iron, oxygen, and silisium decrease, while the amounts of nitrogen and carbon increase exponentially throughout the dendrimer-coating process. The decrease in the levels of iron, oxygen, and silisium atoms was due to the increase of the thickness of PAMAM layers at the surface of the nanoparticles.

The inverted light microscopy images demonstrated that DcMNPs were successfully taken up by MCF-7 cells, even at low concentrations (Wuang et al. 2007; Mahmoudi et al. 2009). The main mechanism for the cellular internalization of MNPs is probably endocytosis (Gupta and Wells 2004).

MCF-7 cells were treated with bare iron oxide nanoparticles, and DcMNPs. Bare iron oxide nanoparticles were not taken up by the cells because of their negative surface charge coming from the abundant OH^- ions which was also demonstrated by Pan et al. (2007). After MNPs were modified with different generations of PAMAM dendrimers, the positive charge increases with respect to the generation number because of the increasing amount of $-NH_3^+$ on the nanoparticle surface. XPS results showed that the amount of positively charged amine groups on the surface of DcMNPs was increased by dendrimer coating (Fig. 8). Positively charged DcMNPs will be easily attached to negatively charged cell membrane which will result in increased rate of cellular internalization. (Figs. 9, 10). In the literature, there are parallel reports (Thorek and Tsourkas 2008; Slowing et al. 2006).

The performed cytotoxicity assays demonstrated that G_7DcMNPs and G_4DcMNP were nontoxic up to 120 and 250 μg ml^{-1} concentrations, respectively. The lower toxicity of G_4DcMNP was due to the fewer number of amine groups at the surface compared with G_7DcMNPs (Table 1). High generations of DcMNPs having abundant functional groups are usually used for ds RNA and oligo nucleotide delivery systems (Boas et al. 2001; Svenson and Tomalia 2005). Pan et al. (2007) demonstrated that G_5DcMNPs could efficiently be used as delivery system for antisense surviving oligodeoxynucleotide (asODN) at 25 ug ml^{-1} concentration in cancer therapy. The toxicity observed at higher generations can be reduced by binding with such ligands. The lower generations of DcMNPs were generally used as drug delivery systems because of their highly branched and multicavity structures. Furthermore, the free amine functional groups in drug-loaded DcMNPs can be modified with different molecules like folic acid (Thomas et al. 2005) and PEG (Tang et al. 2012; Singh et al. 2008) to reduce their cytotoxicity.

The synthesis of DcMNPs for biomedical purposes such as targeted drug delivery is a fairly novel subject. Pan et al. (2005) have synthesized dendrimers up to generation levels of 3.5, 4, and 5. However, they did not perform a detailed investigation on the characterizations and cellular internalizations of nanoparticles. In this study, generation levels of dendrimer up to 7 were synthesized and studied. Also, a detailed investigation was performed for characterization of the dendrimer-coated nanoparticles by XRD, XPS, FTIR, TEM, DLS, ζ potential, VSM, and TGA-FTIR analyses. The cellular internalizations of nanoparticles were also examined by inverted light and confocal microscopy. The synthesis optimization and detailed characterizations on different generations of dendrimer-coated nanoparticles have not been reported in

the literature before. The synthesized dendrimers at different generations can be used for various purposes such as targeted drug delivery, MRI, or hyperthermia. For example, smaller generations of dendrimers can be used as drug carriers, and the greater generations can be used to carry DNA and siRNA molecules by their rigid surface characteristics (Svenson and Tomalia 2005).

It was demonstrated that the synthesized PAMAM coated iron oxide nanoparticles could be suitable as potent drug delivery and magnetic targeting systems when loaded with therapeutics such as anticancer agents. In future studies, the anti cancer agents would be loaded to these MNPs, and drug release, stability, and targetting properties would be evaluated by in vitro and in vivo studies. These MNPs could also be used in chemical separation processes such as protein purifications (Uzun et al. 2010), and environmental pollution control studies(Chou and Lien 2011).

Acknowledgments The support of Asst. Prof. Dr. Bora Mavis for FTIR, as well as financial support by TÜBİTAK-2215 (PhD Fellowship for foreign citizens), is gratefully acknowledged.

References

Acharya S, Dilnawaz F, Sahoo SK (2009) Targeted epidermal growth factor receptor nanoparticle bioconjugates for breast cancer therapy. Biomaterials 30:5737–5750

Arias JL, Gallardo V, Gómez-Lopera SA, Plaza RC, Delgado AV (2001) Synthesis and characterization of poly(ethyl-2-cyanosilane) nanoparticles with a magnetic core. J Control Release 13:309–321

Bazylinski DA (1996) Controlled biomineralization of magnetic minerals by magnetotactic bacteria. Chem Geol 132:191–198

Boas U, Karlsson AJ, de Waal BF, Meijer EW (2001) Synthesis and properties of new thiourea-functionalized poly(propylene imine) dendrimers and their role as hosts for urea functionalized guests. J Org Chem 66(6):2136–2145

Chou CM, Lien HL (2011) Dendrimer-conjugated magnetic nanoparticles for removal of zinc (II) from aqueous solutions. J Nanopart Res 13(5):2099–2107

Du X, Poltorak A, Wei Y, Beutler B (2000) Three novel mammalian toll like receptors: gene structure, expression, and evolution. Eur Cytokine Netw 11(3):362–371

Duncan R, Izzo L (2005) Dendrimer biocompatibility and toxicity. Adv Drug Deliv Rev 57:2215–2237

Durmus Z, Kavas H, Toprak MS, Baykal A, Altınçekiç TG, Aslan A, Bozkurt A, Coşgun S (2009) L-lysine coated iron oxide nanoparticles: synthesis, structual and conductivity characterization. J Alloy Compd 484(1–2):371–376

Esfand R, Tomalia DA (2001) Poly(amidoamine) (PAMAM) dendrimers: from biomimicry to drug delivery and biomedical applications. Drug Discov Today 6:427–436

Gao F, Pan BF, Zheng WM, Ao LM, Gu HC (2005) Study of streptavidin coated onto PAMAM dendrimer modified magnetite nanoparticles. J Magn Magn Mater 293:48–54

Gupta AK, Wells S (2004) Surface-modified superparamagnetic nanoparticles for drug delivery: preparation, characterization, and cytotoxicity studies. IEEE Trans Nano Biosci 3:66–73

Gurdag S, Khandare J, Stapels S, Matherly LH, Kannan RM (2006) Activity of dendrimer-methotrexate conjugates on methotrexate-sensitive and -resistant cell lines. Bioconjug Chem 17:275–283

Hansson GK, Edfeldt K (2005) Toll to be paid at the gateway to the vessel wall. Arterioscler Thromb Vasc Biol 25(6): 1085–1087

Hoa LTM, Dung TT, Danh TM, Duc NH, Chien DM (2009) Preparation and characterization of magnetic nanoparticles coated with polyethylene glycol. J Phys 187(1):012048. doi:10.1088/1742-6596/187/1/012048

Hong S, Bielinska AU, Mecke A, Keszler B, Beals JL, Shi X, Balogh L, Orr BG, Baker JR Jr, Banaszak-Holl MM (2004) Interaction of poly(amidoamine) dendrimers with supported lipid bilayers and cells: hole formation and the relation to transport. Bioconjug Chem 15:774–782

Julian JM, Anderson DG, Brandau AH, McGinn JR, Millon AM (1991) In: Brezinski DR (ed) An infrared spectroscopy atlas for the coatings industry 1 federation of societies for coating technology, 4th edn. Blue Bell, Pennsylvania Vols I and II

Kukowska-Latallo JF, Candido KA, Cao Z, Nigavekar SS, Majoros IJ, Thomas TP, Balogh LP, Khan MK, Baker JR Jr (2005) Nanoparticle targeting of anticancer drug improves therapeutic response in animal model of human epithelial cancer. Cancer Res 65:5317–5324

Lee CC, MacKay JA, Fréchet JM, Szoka FC (2005) Designing dendrimers for biological applications. Nat Biotechnol 23: 1517–1526

Lee CC, Gillies ER, Fox ME, Guillaudeu SJ, Fréchet JM, Dy EE, Szoka FC (2006) A single dose of doxorubicin-functionalized bow-tie dendrimer cures mice bearingC-26 colon carcinomas. Proc Natl Acad Sci USA 103:16649–16654

Liu WM, Xue YN, He WT, Zhuo RX, Huang SW (2011) Dendrimer modified magnetic iron oxide nanoparticle/DNA/PEI ternary complexes: a novel strategy for magnetofection. J Control Release 152:159–160

Mahmoudi M, Simchi A, Milani AS, Stroeve P (2009) Cell toxicity of superparamagnetic iron oxide nanoparticles. J Colloid Interface Sci 336(2):510–518

Majoros IJ, Keszler B, Woehler S, Bull T, Baker JR Jr (2003) Acetylation of poly(amidoamine) dendrimers. Macromolecules 36:5526–5529

Malik N, Evagorou EG, Duncan R (1999) Dendrimer-platinate: a novel approach to cancer chemotherapy. Anticancer Drugs 10:767–776

Malik N, Wiwattanapatapee R, Klopsch R, Lorenz K, Frey H, Weener JW, Meijer EW, Paulus W, Duncan R (2000) Dendrimers: relationship between structure and biocompatibility in vitro, and preliminary studies on the biodistribution of 125I-labelled polyamidoamine dendrimers in vivo. J Control Release 65:133–148

Matsumura Y, Maeda H (1986) A new concept for macromolecular therapeutics in cancer chemotherapy: mechanism

of tumoritropic accumulation of proteins and the antitumor agent smancs. Cancer Res 46:6387–6392

Matsunaga T, Sato R, Kamiya S, Tanaka T, Takeyama H (1999) Chemiluminescence enzyme immunoassay using protein A-bacterial magnetite complex. J Magn Magn Mater 194:126–131

Menjoge AR, Kannan RM, Tomalia DA (2010) Dendrimer-based drug and imaging conjugates: design considerations for nanomedical applications. Drug Discov Today 15(5–6):171–185

Mornet S, Vekris A, Bonnet J, Duguet E, Grasset F, Choy JH, Portier J (2000) DNA–magnetite nanocomposite materials. Mater Lett 42:183–188

Pan BF, Gao F, Gu HC (2005) Dendrimer modified magnetite nanoparticles for protein immobilization. J Colloid Interface Sci 284(1):1–6

Pan B, Cui D, Sheng Y, Ozkan C, Gao F, He R, Li Q, Xu P, Huang T (2007) Dendrimer-modified magnetic nanoparticles enhance efficiency of gene delivery system. Cancer Res 67:8156–8163

Rahman O, Mohapatra SC, Ahmad S (2012) Fe_3O_4 inversespinal super paramagnetic nanoparticles. Mater Chem Phys 132:196–202

Reetz MT, Zonta A, Vijayakrishnan V, Schimossek K (1998) Entrapment of lipases in hydrophobic magnetite-containing sol–gel materials: magnetic separation of heterogeneous biocatalysts. J Mol Catal A 134:251–258

Sato N, Kobayashi H, Hiraga A, Saga T, Togashi K, Konishi J, Brechbiel MW (2001) Pharmacokinetics and enhancement patterns of macromolecular MR contrastagents with various sizes of polyamidoamine dendrimer cores. Magn Reson Med 46:1169–1173

Shimomura M, Abe T, Sato Y, Oshima K, Yamauchi T, Miyauchi S (2003) Sugar-binding property of magnetite particles modified with dihydroxyborylphenyl groups via graft polymerization of acrylic acid. Polymer 44:3877–3882

Shukla R, Thomas TP, Peters J, Kotlyar A, Myc A, Baker JR Jr (2005) Tumor angiogenic vasculature targeting with PAMAM dendrimer RGD conjugates. Chem Commun (Camb) 14:5739–5741

Shukoor MI, Natalio F, Ksenofontov V, Tahir MN, Eberhardt M, Theato P, Schröder HC, Müller WE, Tremel W (2007) Double-stranded RNA polyinosinic polycytidylic acid immobilized onto gamma-Fe_2O_3 nanoparticles by using a multifunctional polymeric linker. Small 3(8):1374–1378

Singh P, Gupta U, Asthana A, Jain NK (2008) Folate and folate-PEG PAMAM dendrimers: synthesis, characterization, and targeted anticancer drug delivery potential in tumor bearing mice. Bioconjug Chem 19(11):2239–2252

Slowing I, Trewyn BG, Lin VS (2006) Effect of surface functionalization of MCM-41-type mesoporous silica nanoparticles on the endocytosis by human cancer cells. J Am Chem Soc 128(46):14792–14793

Stiriba SE, Frey H, Haag R (2002) Dendritic polymers in biomedical applications: from potential to clinical use indiagnostics and therapy. Angew Chem Int Ed Engl 41: 1329–1334

Svenson S (2009) Dendrimers as versatile platform in drug delivery applications. Eur J Pharm Biopharm 71:445–462

Svenson S, Tomalia DA (2005) Dendrimers in biomedical applications reflections on the field. Adv Drug Deliv Rev 57(15):2106–2129

Takeda K, Kaisho T, Akira S (2003) Toll-like receptors. Annu Rev Immunol 21:335–376

Tang Y, Li YB, Wang B, Lin RY, van Dongen M, Zurcher DM, Gu XY, Banaszak Holl MM, Liu G, Qi R (2012) Efficient in vitro siRNA delivery and intramuscular gene silencing using PEG-modified PAMAM dendrimers. Mol Pharm 9(6):1812–1821

Tanyolaç D, Özdural AR (2000) Preparation of low-cost magnetic nitrocellulose microbeads. React Funct Polym 45:235–242

Taylor JI, Hurst CD, Davies MJ, Sachsinger N, Bruce IJ (2000) Application of magnetite and silica–magnetite composites to the isolation of genomic DNA. J Chromatogr A 890:159–166

Thomas TP, Patri AK, Myc A, Myaing MT, Ye JY, Norris TB, Baker JR Jr (2004) Invitro targeting of synthesized antibody conjugated dendrimer nanoparticles. Biomacromolecules 5:2269–2274

Thomas TP, Majoros IJ, Kotlyar A, Kukowska-Latallo JF, Bielinska A, Myc A, Baker JR Jr (2005) Targeting and inhibition of cell growth by an engineered dendritic nanodevice. J Med Chem 48(11):3729–3735

Thorek DL, Tsourkas A (2008) Size, charge and concentration dependent uptake of iron oxide particles by non-phagocytic cells. Biomaterials 29(26):3583–3590

Tomalia DA, Baker H, Dewald J, Hall M, Kallos G, Martin S, Roeck J, Ryder J, Smith P (1985) A new class of polymers: starburst-dendritic macromolecules. Polym J 17:117–132

Unsoy G, Yalcın S, Khodadust R, Gunduz G, Gunduz U (2012) Synthesis optimization and characterization of chitosan-coated iron oxide nanoparticles produced for biomedical applications. J Nanopart Res 14:964

Uzun K, Çevik E, Şenel M, Sözeri H, Baykal A, Abasıyanık FM, Toprak SM (2010) Covalent immobilization of invertase on PAMAM-dendrimer modified superparamagnetic iron oxide nanoparticles. J Nanopart Res 12(8):3057–3067

Wuang SC, Neoh KG, Kang ET, Pack DW, DE Leckband (2007) Synthesis and functionalization of polypyrrole-Fe3O4 nanoparticles for applications in biomedicine. J Mater Chem 17:3354–3362

Zhuo RX, Du B, Lu ZR (1999) In vitro release of 5 fluorouracil with cyclic core dendritic polymer. J Control Release 57:249–257